THE POSSIBILITY OF Na SUBSTITUTION FOR Li ON THE MANGANNESE OXIDES USED AS CATHODE ELECTRODES IN ALKALINE ION BATTERIES

Ta Anh Tan, Le Huy Son

Hanoi Metropolitan University

Abstract: *Li-ionized Ni (LiNi0.1Mn1.9O4) material was synthesized at 700°C by the sol-gel method from lithium acetate, manganese acetate and nickel acetate. The XRD spectrum confirms the spinel-derived samples of LiNi0.1Mn1.9O4 without any impurities. SEM images confirm that the materials were formed in particles with several dozen nanometers. The ion conductivity reached σtp = 19.773×10-5 S.cm-1, the maximum discharge capacity was 85.5 mAh/g and 79.7 mAh/g, respectively. This value is about 70% of theoretical capacity. Materials based on hydroxide manganese oxide synthesized by the hydrothermal method at 205 °C and then annaealed at 600 °C for re-crystallized leaded to nanowire form with a size of 30 nm and a length of several hundred nm to several μm. The ion conductivity is σtp = 31.661×10-5 S.cm-1. Results of the discharge test of the Na0.44MnO2 cathode electrodes in the sodium ion battery configuration showed highest charge and discharge capacities. They were 67.5 mAh/g and 65.8 mAh/g, respectively. Capacity is maintained around 85.3% after 50 cycles. The Coulomb performance reaches 90% in 70 cycles.*

Keywords*: Nanowires, LiNi0,1Mn1,9O4, Na0.44MnO2,ion battery alkaline.*

Received 16.12.2020; accepted for publication 18.1.2021

Email: tatan@daihocthudo.edu.vn

1. INTRODUCTION

Over the last two decades, the spinel materials of transition metal oxides, particularly the $LiMn_2O_4$ compound, has received great attention in the field of lithium ion battery research (LIBs). With its popularity, non-toxic spinel material $LiMn_2O_4$ has more advantages compered to $LiCoO_2$ materials [1, 2]. $LiMn_2O_4$ has a spinel-structured with an Fd-3m space group in which the oxygen atoms formed a compact cube network where the Li ion occupies

tetrahedral sites and the Mn ion occupies octahedral positions. The Li^+/Li charge exiting process (Lithium ion battery) occurs at approximately 4 V (Li^+/Li) [3]. This gives a huge advantage for making LIBs with higher voltages than other anode electrodes. In addition, because of the structural characteristics in its network, there exist three-dimensional conduct that facilitate lithium ion exposures. Moreover, many studies have shown that the $LixMn_{2-x}O_4$ material system can exchange lithium ion with a varying content of x = 1.0 to 0.1 but does not disrupt its structure [4]. $LiMn_2O_4$ also has other advantages such as high operating temperature threshold, high charge rate with high power density. This has the potential to make high-performance, high-density LIBs that meet the requirements for use in electric cars or in renewable energy systems.

The main problem of $LiMn_2O_4$ is the very rapid reduction in volume after the first cycle at both room temperature and high temperature. Decline in storage capacity or during lifecycle phases is not well defined, many of which could be suggested as: structural rigidity; network distortion effect Jahn-Teller [5]; Mn dissolved in electrolyte solution, … To solve this problem, the research focuses on partially replacing metal ions of Co, Ni, Al, Mg, Cr, Fe, ... into Mn or replacing F or S into one. The position of the oxides [6, 7] to improve the capacity as well as the stability of the discharge cycles. Among these alternative materials, $LiNixMn_{2-x}O_4$ shows the best charge/discharge stability. This improvement may be due to the similarity of ionic radius of Ni to Mn and the strong chemical bond of Mn-O-Ni to stabilize the octagonal spinel, Mn^{3+} into the electrolyte and limiting the Jahn-Teller effect [8].

Another interesting issue that is of great interest recently is the replacement of Li^+ ion with Na^+ ion in the compound with MnO_2 oxide [9, 10] or V_2O_5 [11, 12]. It creates sodium ion exchange resins and is used to manufacture sodium ion batteries (NIBs: Natrium ion batteries), also known as sodium ion batteries. This is a new research direction and NIBs are emerging as a candidate for replacing lithium ion batteries in a number of areas, particularly in the field of large-scale energy storage. NIBs have many advantages, such as low cost, due to the large volume of sodium in the earth's crust, easy to manufacture and environmentally friendly.

In this paper, we compare the electrical and electrochemical properties of materials. Materials Li based on manganese oxide nanoparticles ($LiNi_{0.1}Mn_{1.9}O_4$) were synthesized at 700°C by the method sol-gel from lithium acetate, acetate manganese and nickel acetate with manganese oxide based on hydrothermal materials at 205°C and then re-crystallized at 600°C. The purpose of it is that assessing the possibility of Na substitution for Li on conducting material.

2. EXPERIMENTAL

2.1.Manufacture materials: $LiNi_{1,1}Mn_{1,9}O_4$

Firstly, mix at the atomic ratio of Li : Ni : Mn = 1 : 0.1 : 1.9 of lithium acetate, manganese acetate and acetate acetate are dissolved in deionized water separately for each substance (water content is calculated according to the solubility of component materials) and stirring for 1 hour to dissolve, then they are mixed and stirred for 1 hour to mix well. Secondly, citric acid was added to the proportional solution solution (Li : Mn : citric acid = 1 : 2 : 3) [13]. The mixture was stirred for 10 hours at 80° C and a white gel was formed. During this process the pH was maintained at 7.0 by adding NH_3OH to the mixture [13]. The resulting gel mixture was dried in air at 15 hours at 120°C. The collected material is crushed by a mortar for 2 hours. The material after milling is sintered at 700°C.

2.2.Manufacture materials: $Na_{0.44}MnO_2$

Materials $Na_{0.44}MnO_2$can be used in many different ways such as hydrothermal [39]; The solid stated reaction; sol-gel; ... In this work, we choose to synthesize $Na_{0.44}MnO_2$ via hydrothermal method. Because in recent publications, the $Na_{0.44}MnO_2$ nanoparticle composite prepared by the hydrothermal method had good electrochemical activities. It gives a higher capacity, larger discharge current densities and longer shelf life.

Initially, 2 grams of Mn_2O_3 material was dissolved in 80 ml of 5M NaOH and stirred for the material to be thoroughly mixed. The mixture was then placed in an Autoclave with 120 ml Teflon and heated for 96 hours at 205°C. Then, the material is cooled naturally. The mixture was reconstituted in deionized water, stirring for 1 hour then ultrasonic vibration for 1 hour. Next the material is washed several times with deionized water and centrifuged to remove excess NaOH. The collected material was dried under vacuum for 10 hours at 120°C. Then a portion of this material was annealed at 600°C in air with a heating rate of 10°/min and continuous anealing for 6 hours. The final material is cooled naturally.

Structural characteristics of the materials were studied on the X-ray diffraction system - D5005SIEMEN with Cu Kα emission source (λ = 1.5406 Å). Morphological characteristics were investigated on the FE-SEM HITACHI 4800 scanning electron microscope.

Thin film electrodes are made from $LiNi_{0.1}Mn_{1.9}O_4$ ($Na_{0.44}MnO_2$) material mixed with carbon black (super P and KS4) and polyvinylidenefluoride (PVDF) in N-methylpyrrolidone (NMP) 70:20:10. This solution is coated on a thin sheet of aluminum 15 μm thick and then dried at 100°C by vacuum for 12 hours to obtain a cathode leaf.

The cathode is then pressed using roller presses and hydraulic presses to increase density and uniformity, followed by cutting into circular electrodes that use positive electrode in the CR203 battery.

The ionic charge/discharge corresponds to the charge that occurs in the battery at the side cathode electrode. Load measurements for Li ion conductive materials were performed with CR203 cathode-ray anode using SnO_2 tin oxide, polyethylene-polypropylene-polyethylene separating membrane, $LiClO_4$ 1M electrolyte solution in Solvent ethylene carbonate/diethylene carbonate.

3. RESULTS AND DISCUSSION

3.1.The structure and morphology of the materials

Figure 1 showed the x-ray diffraction pattern of the Li-ion-conducting material on a manganese oxide base synthesized by sol-gel method. It showed that all diffraction peaks in JPCDS No. 35-0782 with a spinel structure $LiMn_2O_4$ material and absolutely no peak of any other substance. Thus, when we doped Ni with a molecular weight of 0.1, then the nickel ion completely occupies the positions of the ion Mn in the spinel crystal lattice. This is again confirmed by the Raman scattering results of the fabricated material. Figure 2a is the Raman scattering of $LiMn_2O_4$ and Figure 2b is of the produced sample $LiNi_{0.1}Mn_{1.9}O_2$. Raman scattering has the ability to analyze the structure at the molecular level as well as investigate the proximity of cations and complex anions in transition metal oxides. According to Ammundsen et al [14]. the oscillations of the AB_2O_4 spinel material are described as follows:

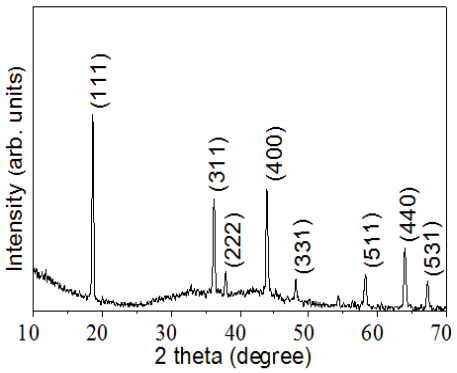

Figure 1. *XRD spectra of* $LiNi_{0.1}Mn_{1.9}O_2$

$\Gamma = A_{1g} + E_g + E_{1g} + 3F_{2g} + A_{2u} + 2E_u + 4F_{1u} + 2F_{2u}$ ([15-17])

The oscillator types include: i) symmetric strain (A_{1g}); ii) symmetric deformation (E_g); iii) three types of symmetric bending distortion (F_{2g}), which are Raman scattering patterns and can be observed in the Raman spectra; iv) four types of asymmetrical stretching or bending (F_{1u}) oscillations only visible on IR spectra [16].

Although five Raman oscillators are predicted for spinel $LiMn_2O_4$, however, the Raman spectra of different materials are different due to different spatial symmetry groups. Spinel

$LiMn_2O_4$ usually has a disordered structure of Fd-3m due to the relatively high conductivity of the material. In Figure 2, the Raman spectra of the $LiMn_2O_4$ spinel is a large and strong region (Mn-O tension strain) at ~ 620 cm^{-1} with a small peak at ~ 580 cm^{-1}. They are closely related to the octahedral MnO_6 and the oxidation state of Mn, respectively called A_{1g} and $F_{2g}^{(1)}$ [15]. The expansion of the A1g region is due to the small difference in the octahedral $Mn^{4+}O_6$ octahedral structure and the octahedral $Mn^{3+}O_6$ is partially distorted in $LiMn_2O_4$. Its intensity depends on the concentration of Mn^{4+} in the material and reflects the average oxidation state of Mn. For this reason, according to Yingjin Wei et al. [15], the regions A1g and $F_{2g}^{(1)}$ are not separated in unmodified $LiMn_2O_4$ because the concentrations of Mn^{3+} and Mn^{4+} are equal in the material. Then $F_{2g}^{(1)}$ is noticeable with the substitution of Ni and the range A_{1g} becomes distinct and sharper from the region $F_{2g}^{(1)}$. The change in A_{1g} and $F_{2g}^{(1)}$ with the replacement of Ni is consistent with the increase in Mn^{4+} concentration as well as the increase of Mn oxidation state in $LiNi_xMn_{2-x}O_4$. Peak $F_{2g}^{(1)}$ derives primarily from the oscillation of the Mn^{4+}- O bond. Its intensity depends on the concentration of Mn^{4+} in the material reflecting the average oxidation state of Mn. As shown in Fig. 2a, the regions A_{1g} and $F_{2g}^{(1)}$ are not separated in the non-doped sample $LiMn_2O_4$ due to the concentration of Mn^{3+} and Mn^{4+} in the same material (Mn^{3+} : Mn^{4+} = 1 : 1).

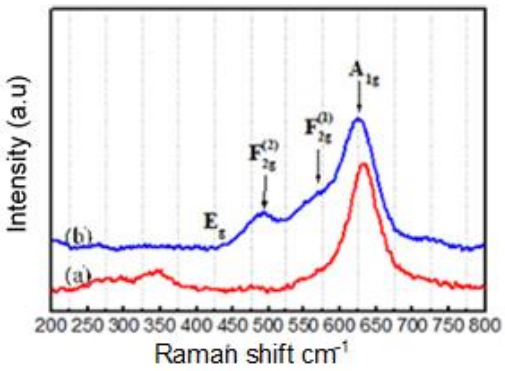

Figure 2. *Raman spectra of LiMn2O4 (a) and $LiNi_{0.1}Mn_{1.9}O_4$ (b).*

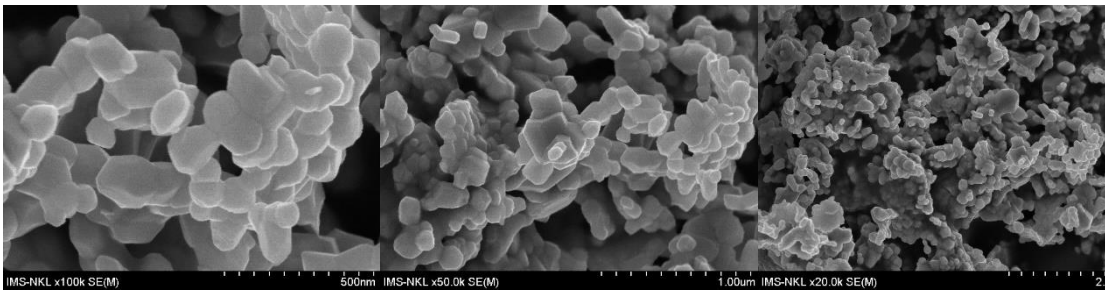

Figure 3. *SEM image of material $LiNi_{0.1}Mn_{1.9}O_4$*

Figure 3 shows that the material $LiNi_{0.1}Mn_{1.9}O_4$ was made with uniform morphology and size of 200 nm.

The X-ray diffraction pattern of the manganese oxide based ion-conducting material synthesized by hydrothermal method from Mn_2O_3 and NaOH precursors at 205°C is shown in Figures 4a. The process of searching and quantifying phases in materials is done by QualX software using both databases including open source databases (COD) and commercial PDF databases (JCPDF). The observation shown in Figure 4a shows that the XRD spectrum of the sample showed no presence of the manganese oxide material. Instead, a rich Na-phase was obtained with a $Na_{0.7}MnO_{2.05}$ formula. This phase appearance may be due to excess Na diffusion into the $Na_{0.44}$ MnO_2 network.

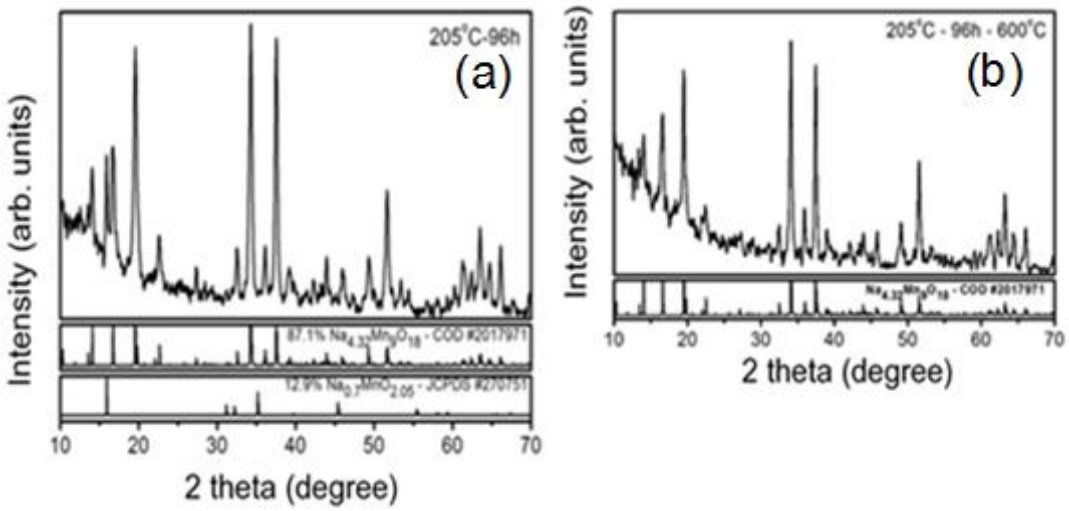

Figure 4. *XRD diagram of hydroxylated Na_xMnO_2 at 205°C (a) and post-crystallization (b)*

By observing the excess Na in the hydrothermal sample at 205°C for 96 hours, we used a thermal treatment in the hope of producing a single-phase material and a more stable crystalline structure. In Figure 4b, the diffraction spectrum of the hydrothermal material at 205°C for 96 hours is then tempered at 400 °C for a period of 6 hours, where the vertices belong to the $Na_{0.58}Mn_2O_41.5H_2O$ phase. completely disappeared and only the diffraction peaks of the $Na_{0.44}MnO_2$ phase were observed in the XRD scheme. Thus, the $Na_{0,44}MnO_2$ sample was made by hydrothermal method at 205°C for 96 hours and then incubated at 600°C for 6 hours.

Figure 5 shows that the $Na_{0.44}MnO_2$ material was made by hydrothermal heat at 205°C for 96 hours completely morphologically in the form of nanowires with a size of 50 nm and a few tens of μm. After recrystallisation at 400°C for 4 hours, the nanoparticles were sized at 50 nm and 5 μm long.

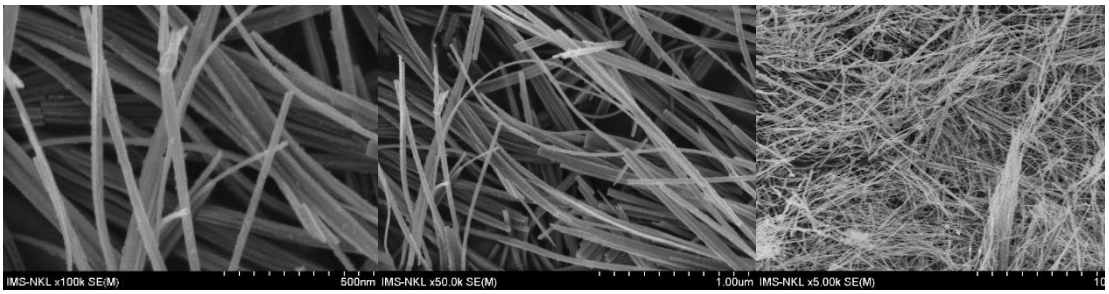

Figure 5. *Sample SEM image is made of hydrothermal energy at 205 °C.*

3.2. Electrical and electro chemical properties of materials.

The ionic conductivity of the synthesized materials was studied by electrochemical total impedance spectroscopy. Samples were prepared by cold-kneading at 40 MPa to produce cylindrical tablets with a 12 mm diameter profile and 1.5 mm thick. The electrode of the pellets was prepared by evaporation of gold onto a cylindrical tube with a diameter of 10 mm and a thickness of 1 μm. Total impedance spectral measurements were performed by Autolab measuring system at 10mV amplitude and frequency range 10^{-1} to 10^{6} Hz. To match the data we use Nova software provided by Autolab.

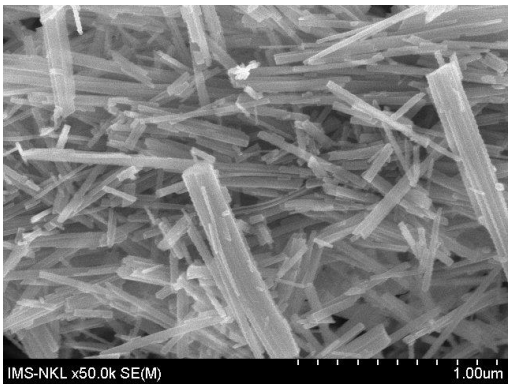

Figure 6. *SEM images of hydrolysed samples after incubation*

The results of calculating the lithium ion conductance of the $LiNi_xMn_{2-x}O_4$ composite by sol-gel method through the impedance spectral spectrometry of clamp solid electrode showed the lithium conductivity of $LiNi_{0.1}Mn_{1.9}O_4$ is $\sigma_{tp} = 19.773\times10^{-5}$ S.cm^{-1} and the ionic conductivity of $Na_{0.44}MnO_2$ is $\sigma_{tp} = 31.661\times10^{-5}$ S.cm^{-1}. This conductivity value is similar to a number of studies reported [18, 19]. Both materials give high ionic conductivity because nanoparticles are made of materials. Distortion of the grain boundaries results in high ionic conductivity.

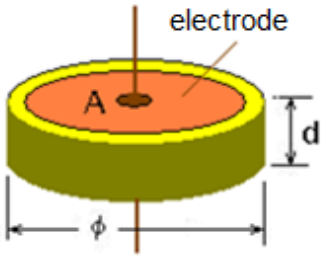

Figure 7. *Two-electrode sample*

Figure 7 shows the results of the charging/discharging capacity of the cathode electrode as thin film electrode from $LiNi_{0.1}Mn_{1.9}MnO_4$ material with positive SnO_2

electrode in 1M $LiClO_4$ electrolyte for discharge capacity of 79.7 mAh/g. Thus, $LiNi_xMn_{2-x}O_4$ substitute material for Ni for Mn with x = 0.1 ratio improved electrochemical performance better than non-Ni substitute material.

Figure 8 illustrates the charging/discharging curves in cycles 1, 10, and the 20th cycle with currents of 0.1 C; Voltage 2.0 ÷ 4.0 V. The discharge capacity of cycle 1; 10 and cycle 20 are 62.7 mAh/g, 64.0 mAh/g and 65.8 mAh/g respectively. These values are equivalent to the volume of $Na_{0,44}MnO_2$ material coated with surface carbon [20]. The first discharge capacity of the $Na_{0,44}MnO_2$/C material is about 80 mAh/g. The higher $Na_{0.44}MnO_2$/C content may be due to the higher carbon conductivity on the surface of $Na_{0.44}MnO_2$ particles compared to the non-carbonated $Na_{0.44}MnO_2$ particles.

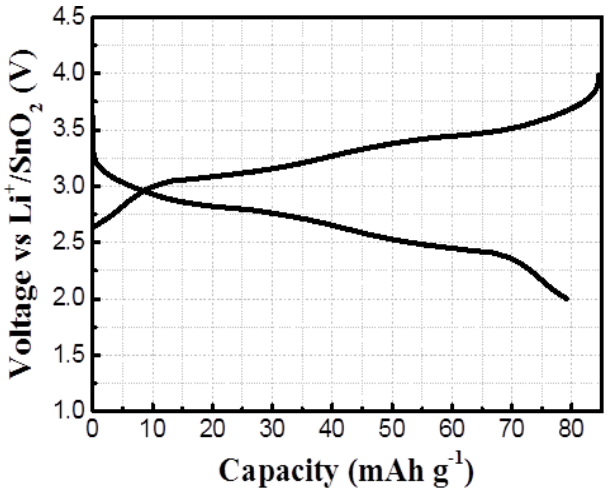

Figure 8. *Charge/discharge curve of $LiNi_{0.1}Mn_{1.9}MnO_4$ material.*

It can be seen that both charge and discharge curves exhibit voltage stabilization demonstrations that the $Na_{0.44}MnO_2$ material has been phase-shifted during the sodium ion injection into the material structure. The similarly charged/discharged curves of $Na_{0.44}MnO_2$ material were also published by other research groups [21, 22]. Based on the published results, the CV (CV) spectra of $Na_{0.44}MnO_2$ material consist of six pairs of redox stress peaks, corresponding to six different inlet/outlet steps of sodium ion in structure of $Na_{0.44}MnO_2$ [20, 21, 23].

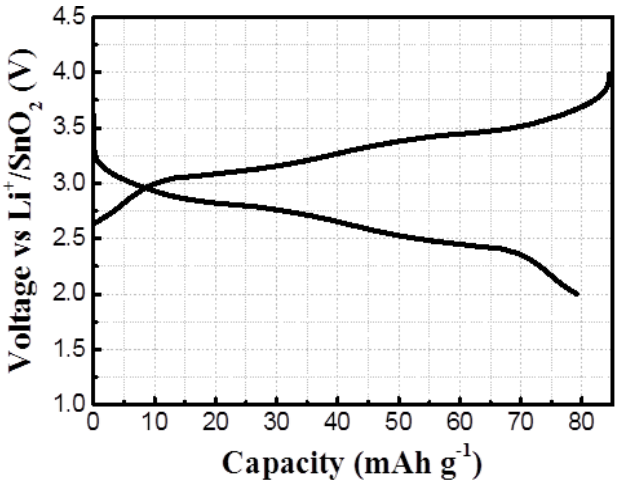

Figure 9. *The first, 10th, and 20th discharge curves of cathode material Na0.44MnO2 at 0.1 C line current;*

4.CONCLUSION

Thus sol-gel method successfully synthesized $LiNi_{0.1}Mn_{1.9}MnO_4$ nanoparticles developed equally at 200 nm size and hydrothermally synthesized $Na_{0.44}MnO_2$ nano with a size of 50 nm and a few μm in length.

The results of electrical and electrochemical survey showed that the conductivity of $Na_{0.44}MnO_2$ material is $\sigma_{tp} = 31.661\times10^{-5}$ $S.cm^{-1}$ higher than that of $LiNi_{0.1}Mn_{1.9}MnO_4$ material at $\sigma_{tp} = 9{,}773\times10^{-5}S.cm^{-1}$. However, the measured results show that the $LiNi_{0.1}Mn_{1.9}MnO_4$ material has a discharge capacity of 79.7 mAh/g and the $Na_{0.44}MnO_2$ content is only 65.8 mAh/g.

Although the loading capacity of $Na_{0.44}MnO_2$ material is smaller than that of $LiNi_{0.1}Mn_{1.9}MnO_4$ material. In practice, however, the theoretical capacity of the Na ion conducting material is less than the theoretical capacity of the Li ion conducting material on the manganese oxide base, and the measurement results show the coulomb efficiency of the Na reached 90% and capacity remained stable during 70 cycles. This combined with the Na source and the fence on the Earth leading to the Na-ion conducting material is a bright candidate for the cathode electrode for rechargeable batteries replacing the future sodium ion-carrying material near the.

REFERENCES

1. Cai, Y., et al. (2014), "Long cycle life, high rate capability of truncated octahedral $LiMn_2O_4$ cathode materials synthesized by a solid-state combustion reaction for lithium ion batteries", *Ceramics International*, 40(9, Part A): pp. 14039-14043.
2. Guo, H.-j., et al. (2011), "Novel synthesis of $LiMn_2O_4$ with large tap density by oxidation of manganese powder", *Energy Conversion and Management*, 52(4): pp. 2009-2014.
3. Yang, Z., et al. (2013), "High-performance porous nanoscaled $LiMn_2O_4$ prepared by polymer-assisted sol–gel method". *Electrochimica Acta*, 106: p. 63-68.
4. Li, T., et al. (2007), "Effect of lithium content on the electrochemical properties of solid-state-synthesized spinel $LixMn_2O_4$", *Rare Metals*, 26(3): p. 280-285.
5. Gummow, R.J., A. de Kock, and M.M. Thackeray. (1994), "Improved capacity retention in rechargeable 4 V lithium/lithium-manganese oxide (spinel) cells", *Solid State Ionics*, 69(1): p. 59-67.

6. Amatucci, G., et al. (1990) "The elevated temperature performance of the $LiMn_2O_4$/C system: failure and solutions", *Electrochimica Acta*, 45(1–2): pp. 255-271.
7. Jiang, Q., et al. (2015), "Plasma-Assisted Sulfur Doping of LiMn2O4 for High-Performance Lithium-Ion Batteries", *The Journal of Physical Chemistry C*, 119(52): pp. 28776-28782.
8. Xifei, L., X. Youlong, and W. Chunlei. (2009), "Suppression of Jahn–Teller distortion of spinel $LiMn_2O_4$ cathode", *Journal of Alloys and Compounds*, 479: pp. 310–313.
9. Dai, K., et al. (2015), "$Na_{0.44}MnO_2$ with very fast sodium diffusion and stable cycling synthesized via polyvinylpyrrolidone-combustion method", *Journal of Power Sources*, 285: pp. 161-168.
10. Wang, C.-H., et al. (2015), "Rechargeable Na/$Na_{0.44}MnO_2$ cells with ionic liquid electrolytes containing various sodium solutes". *Journal of Power Sources*, 274: pp. 1016-1023.
11. Moretti, A., et al. (2015), "V_2O_5 electrodes with extended cycling ability and improved rate performance using polyacrylic acid as binder". *Journal of Power Sources*, 293(Supplement C): pp. 1068-1072.
12. Wang, H., et al. (2014), "Nanostructured V_2O_5 arrays on metal substrate as binder free cathode materials for sodium-ion batteries", *Electrochimica Acta*, 182(Supplement C): pp. 769-774.
13. Hwang, B.J., et al. (2001), "Effect of Al-substitution on the stability of $LiMn_2O_4$ spinel, synthesized by citric acid sol–gel method". *Journal of Power Sources*, 102(1–2): pp. 326-331.
14. Ammundsen, B., et al. (1999), "Lattice Dynamics and Vibrational Spectra of Lithium Manganese Oxides: A Computer Simulation and Spectroscopic Study". *The Journal of Physical Chemistry B*, 103(25): pp. 5175-5180.
15. Wei, Y., et al. (2006), "Spectroscopic studies of the structural properties of Ni substituted spinel $LiMn_2O_4$", *Solid State Ionics*, 177(1–2): p. 29-35.
16. Julien, C.M. and M. Massot. (2003), "Lattice vibrations of materials for lithium rechargeable batteries I. Lithium manganese oxide spinel", *Materials Science and Engineering: B*, 97(3): pp. 217-230.
17. Arumugam, D., G.P. Kalaignan, and P. Manisankar. (2008), "Development of structural stability and the electrochemical performances of 'La' substituted spinel $LiMn_2O_4$ cathode materials for rechargeable lithium-ion batteries", *Solid State Ionics*, 179(15–16): pp. 580-586.
18. Smaha, R.W., et al. (2015), "Tuning Sodium Ion Conductivity in the Layered Honeycomb Oxide $Na_{3-x}Sn_{2-x}Sb_xNaO_6$". *Inorganic Chemistry*, 54(16): pp. 7985-7991.
19. Hayashi, A., et al. (2014), "High sodium ion conductivity of glass–ceramic electrolytes with cubic Na_3PS_4". *Journal of Power Sources*, 258(Supplement C): pp. 420-423.
20. Sauvage, F., et al. (2007), "Study of the Insertion/Deinsertion Mechanism of Sodium into $Na_{0.44}MnO_2$". *Inorganic Chemistry*, 46(8): pp. 3289-3294.

21. He, X., et al.(2016), "Durable high-rate capability $Na_{0.44}MnO_2$ cathode material for sodium-ion batteries", *Nano Energy*, 27: pp. 602–610.

22. Hosono, E., et al. (2012), "High power Na-ion rechargeable battery with single-crystalline $Na_{0.44}MnO_2$ nanowire electrode". *Journal of Power Sources*, 217: pp. 43-46.

23. Fu, B., X. Zhou, and Y. Wang. (2016), "High-rate performance electrospun $Na_{0.44}MnO_2$ nanofibers as cathode material for sodium-ion batteries". *Journal of Power Sources*, 310: pp. 102-108.

KHẢ NĂNG THAY THẾ CỦA VẬT LIỆU Na CHO Li TRÊN NỀN MANGAN OXIT ĐỂ SỬ DỤNG LÀM ĐIỆN CỰC CATOT CHO PIN ION KIỀM

Tóm tắt: *Vật liệu Li trên nền mangan oxit có pha tạp Ni ($LiNi_{0,1}Mn_{1,9}O_4$) được tổng hợp ở 700°C bằng phương pháp sol-gel từ Liti axetat, mangan axetat và niken axetat. Phổ XRD đã xác nhận các mẫu thu được có cấu trúc spinel của $LiNi_{0,1}Mn_{1,9}O_4$ mà không có bất kỳ tạp chất nào. Ảnh SEM khẳng định vật liệu có dạng hạt với kích thước vài chục nm. Độ dẫn ion đạt σ_{tp} = 19,773.10-5 $S.cm^{-1}$, dung lượng nạp xả đạt giá trị cao nhất tương ứng là 85,5 mAh/g và 79,7 mAh/g. Giá trị này đạt khoảng 70% so với dung lượng lý thuyết. Vật liệu Na trên nền mangan oxit tổng hợp bằng phương pháp thủy nhiệt ở 205°C sau đó ủ nhiệt tái kết tinh ở 600°C cho chúng ta dạng dây nano với kích thước cỡ 30 nm và dài từ vài trăm nm đến vài μm. Độ dẫn ion đạt σ_{tp} = 31,661.10^{-5} $S.cm^{-1}$. Kết quả khảo sát quá trình nạp xả của các dương cực $Na_{0,44}MnO_2$ trong cấu hình pin ion natri cho dung lượng trong quá trình nạp và xả cao nhất tương ứng là 67,5 mAh/g và 65,8 mAh/g. Dung lượng được duy trì khoảng 85,3% sau 50 chu kỳ; hiệu suất culong đạt 90% trong 70 chu kỳ.*

Từ khóa: *Dây nano, $LiNi_{0,1}Mn_{1,9}O_4$, $Na_{0.44}MnO_2$, pin ion kiềm.*